

## Quasi-static cyclic two-way out-of-plane bending tests and analytical models comparison for URM walls

Damiola, Marina; Esposito, Rita; Messali, Francesco; Rots, Jan

**Publication date**

2018

**Document Version**

Accepted author manuscript

**Published in**

Proceeding of the 10th international masonry conference

**Citation (APA)**

Damiola, M., Esposito, R., Messali, F., & Rots, J. (2018). Quasi-static cyclic two-way out-of-plane bending tests and analytical models comparison for URM walls. In G. Milani, A. Taliercio, & S. Garrity (Eds.), *Proceeding of the 10th international masonry conference : Milan, Italy, July 9-11, 2018*

**Important note**

To cite this publication, please use the final published version (if applicable).  
Please check the document version above.

**Copyright**

Other than for strictly personal use, it is not permitted to download, forward or distribute the text or part of it, without the consent of the author(s) and/or copyright holder(s), unless the work is under an open content license such as Creative Commons.

**Takedown policy**

Please contact us and provide details if you believe this document breaches copyrights.  
We will remove access to the work immediately and investigate your claim.

## QUASI-STATIC CYCLIC TWO-WAY OUT-OF-PLANE BENDING TESTS AND ANALYTICAL MODELS COMPARISON FOR URM WALLS

Marina Damiola<sup>1</sup>, Rita Esposito<sup>2</sup>, Francesco Messali<sup>3</sup>, and Jan G.Rots<sup>4</sup>

Delft University of Technology, Faculty of Civil Engineering and Geosciences  
Delft, The Netherlands

{M.Damiola<sup>1</sup>, R.Esposito<sup>2</sup>, F.Messali<sup>3</sup>, J.G.Rots<sup>4</sup>}@tudelft.nl

**Keywords:** Unreinforced masonry, Two-way out-of-plane failure mechanism, Virtual work method, Quasi-static cyclic tests

**Abstract.** *Out-of-plane failure is one of the most important mechanisms for unreinforced masonry (URM) structures to be prevented in the seismic areas. The one-way out-of-plane bending failure mechanism has been studied by several authors. The two-way bending failure mechanism has received much less attention and only few formulations for specific cases are available in standards and in the literature.*

*In order to investigate the two-way bending failure mechanism, four full-scale URM walls were tested quasi-statically. Both calcium silicate and clay brick masonry typical of Dutch building were tested. In comparison with the experimental results, a critical evaluation of the available analytical models proposed by Eurocode 6, the Australian standards and the simplified macroblock approach by Vaculik and Griffith is presented. Despite some limitation in its application and the underestimation in the results, the most promising analytical formulation is the one provided by the Australian standards. In order to provide a basis for the development of an improved formulation for two-way bending, a parametric study on the Australian standard formulation is presented. The parameters that mostly influence the prediction of the bending capacity of the wall are the flexural strength of masonry, the vertical edges rotational restraint coefficient, the aspect ratio, and the wall thickness. On the contrary, the parametric study also shows that variations of the overburden do not lead to variation in terms of capacity.*

## 1 INTRODUCTION

The out-of-plane failure is one of the most important failure mechanisms for masonry structures, often called “first damage mode” [1], to be prevented in the seismic assessment. Within the out-of-plane failure, two main mechanisms can be distinguished: the one-way out-of-plane bending failure and two-way out-of-plane bending failure. The one-way out-of-plane bending failure usually occurs in slender walls not laterally supported and it is characterized by a rapid degradation in capacity that needs to be prevented. Several authors studied this failure mechanism developing an accurate procedure for the one-way out-of-plane seismic response of unreinforced masonry (URM) walls. The two-way out-of-plane bending failure generally occurs in squat walls supported on the sides. It triggers a complex crack pattern that produces less degradation in capacity and more energy dissipation than the one-way failure mechanism. This failure mechanism is less studied with respect to the one-way failure mechanism and only a few formulations for specific cases have been developed. Most of the standards, in fact, do not provide specific recommendations for the two-way bending failure mechanism, and the application of one-way bending models significantly underestimates the walls lateral force capacity.

This paper aims at providing a basis for the development of an improved formulation able to capture the two-way bending failure mechanism. In order to investigate the two-way bending failure mechanism, full-scale URM walls were tested in quasi-static out-of-plane bending at Delft University of Technology [2-4]. The tests have been performed for different masonry types characterized by brick and general purpose mortar according to the features of the Dutch existing URM buildings. In fact, in The Netherlands the majority of buildings consist of URM characterized by limited wall thickness and is not designed for seismic loading, while recently induced seismicity due to gas extraction became a problem in the northern part of The Netherlands. In comparison with the experimental results, a critical evaluation of the available analytical models proposed by Eurocode 6 [5], the Australian standard [6] and the simplified macroblock approach by Vaculik and Griffith [7-8] is presented. Eventually, a parametric study on the most promising analytical formulation by the Australian standard is also presented.

## 2 MATERIALS AND METHOD

In order to investigate the two-way out-of-plane bending failure mechanism, four full-scale URM walls were subjected to quasi-static cyclic out-of-plane tests at Delft University of Technology. Table 1 shows an overview of the tested walls summarizing the type and the size of the masonry units and the geometry of each wall. Detailed information on the tests can be found in Refs. [2-4].

Sample name	Units type	Units size (mm)	Length (mm)	Height (mm)	Thickness (mm)
TUD_COMP-10	Perforated clay brick	210x100x50	4000	2751	100
TUD_COMP-11	Calcium silicate brick	210x100x70	3874	2765	100
TUD_COMP-26	Solid clay brick	210x100x50	3950	2710	100
TUD_COMP-27	Solid clay brick	210x100x50	3840	2710	210

Table 1: Overview of quasi-static cyclic out-of-plane tests.

The characterization of all four masonry types was carried out by performing destructive laboratory tests on both masonry and its constituents in accordance with European standards. For all masonry types, cement-based mortar was used and the thickness of both bed and head joints was 10 mm. The main material properties of units and masonry are summarized in Table 2. Detailed information on the tests can be found in the dedicated reports [9-10].

<u>Material properties (MPa)</u>	Symbol	Perforated clay masonry	Calcium silicate masonry	Solid clay masonry	
				Single wythe	Double wythe
Compressive strength of mortar	$f_m$	6.11 (0.09)	6.59 (0.10)	3.81 (0.09)	
Flexural strength of mortar	$f_{mt}$	2.43 (0.13)	2.79 (0.08)	1.40 (0.12)	
Compressive strength of unit	$f_b$	-	13.26 (0.13)	28.31 (0.10)	
Flexural strength of unit	$f_{bt}$	4.78 (0.20)	2.74 (0.06)	6.31 (0.11)	
Compressive strength of masonry	$f'_m$	14.73 (0.07)	5.93 (0.09)	14.02 (0.04)	9.26 (0.14)
Elastic modulus of masonry in the direction perpendicular to bed joints evaluated as the chord between 1/10 and 1/3 of the maximum stress	$E_3$	8156 (0.16)	2746 (0.10)	4590 (0.13)	2951 (0.15)
Flexural (bond) strength of masonry	$f_w$	0.27 (0.54)	0.27 (0.43)	0.15 (0.32)	
Flexural strength of masonry for a plane of failure perpendicular to the bed joints	$f_{x2}$	1.12 (0.28)	0.76 (0.36)	0.65 (0.28)	0.41 (0.15)

Table 2: Overview material properties (in MPa). The value between brackets corresponds to the coefficient of variation in percentage.

Figure 1 shows the two-way out-of-plane test set-up. Each wall was built within a steel frame composed by two beams placed at the top and bottom of the wall connected via springs to two lateral columns. The wall within its steel frame was placed in the set-up by connecting the top and bottom steel beam to cross beams. At the bottom the cross beams were connected to the transversal beams, while at the top glass plates were installed between the cross beams and the transversal beams to allow the vertical translation of the wall during out-of-plane deformations. Each wall was laterally constrained with hinged connections made of steel tubes. In order to prevent damage due to the interaction between the steel tubes and the masonry wall, wooden wedges were placed in between them.

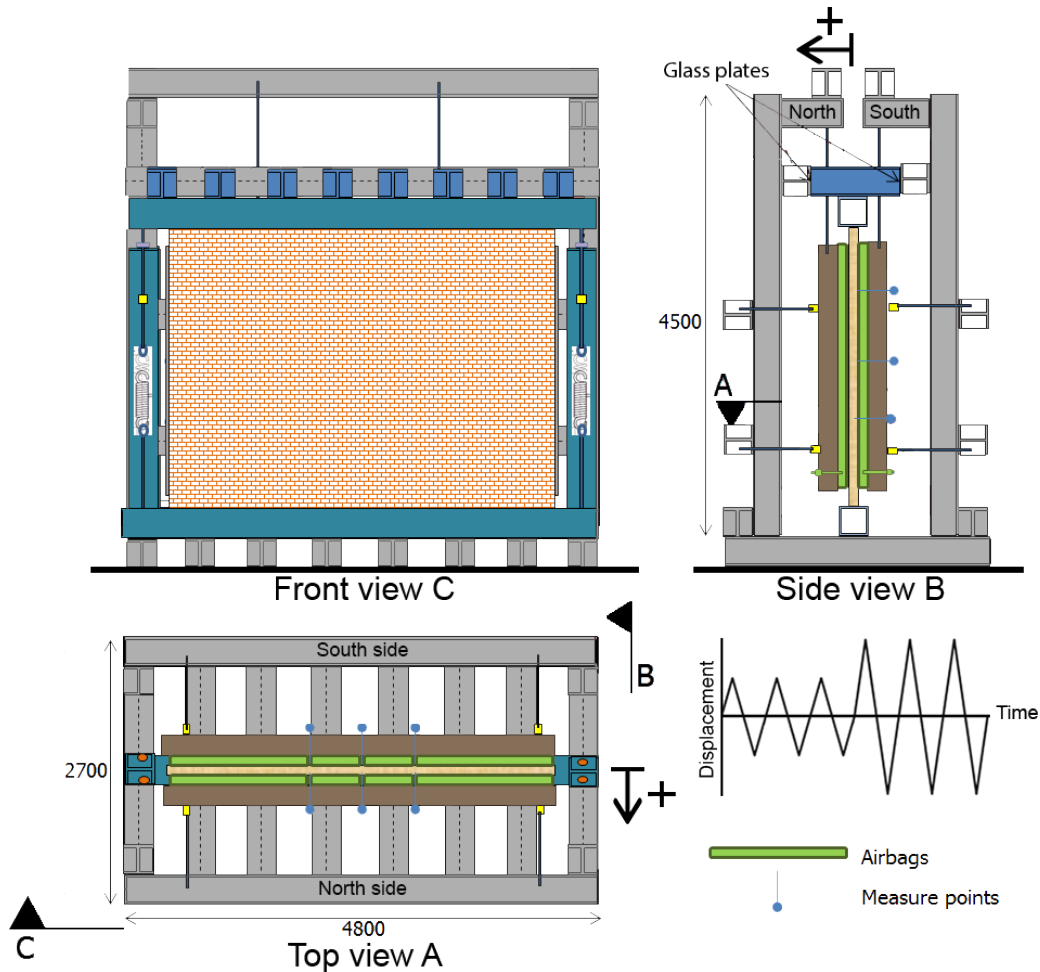


Figure 1: Test set-up for squat walls subject to two-way out-of-plane cyclic tests.

Before the test an overburden of 0.06 MPa was applied (and then maintained constant throughout the test) at the top of each wall by pre-tensioning the four springs connecting the top steel beam and the lateral columns.

A uniform lateral load was applied using airbags on both north and south sides of the wall. On both sides, airbags were pumped up to a certain initial pressure before starting the test. During the test the pressure was kept constant in the airbags on the north side, while it was varying in the airbags on the south side to apply the desired imposed displacement at the center of the wall. The initial pressure was chosen to prevent negative pressure in the airbags placed on the south side. A timber reaction frame was adopted to allow the measurement of the applied load via external load cells. During the test, due to the presence of the airbags and the timber reaction frame, the propagation of the cracks could not be observed.

The net contact area between the wall and the airbags was calculated by comparing the force measured by the load cells  $F_N$  and the pressure measured by the airbags  $P$ , on the north side ( $A_{net}=F_N/P$ ). By considering as a reference the area of the airbags in their uninflated condition  $A_{airbags}$ , it was observed that the net contact area  $A_{net}$  during the test was approximately 75-80% of the reference area. The same range of values is reported by Griffith et al. [11].

The response of the wall was monitored through load cells and linear potentiometers. The former aims at monitoring the applied overburden and recording the lateral force against the timber reaction frame; the latter aims at recording the horizontal displacements of the wall at different locations and monitoring potential rotations. The applied lateral load is calculated as

the difference between the total force measured by the load cells on the south side  $F_S$  and the one measured on the north side  $F_N$ .

The test was performed in displacement control by controlling the displacement of the mid-point. The displacement at the mid-point was cyclically varied (Figure 1). Every cycle was composed by three identical runs. In every run the displacement was first applied in the positive loading direction (from south to north) and afterwards in the negative loading direction (from north to south).

During the testing campaign, an asymmetric response of the wall was recorded in the lateral force versus mid-point displacement (capacity curve); in particular larger forces were recorded for positive displacements. This feature is the result of the adopted loading procedure in which the airbags on both sides of the wall were always inflated. By following the aforementioned loading procedure, a stable control of the imposed displacement can be achieved and sudden instability deformations of the wall are prevented. However, when the wall is subject to bending deformation, the airbags pressure is acting both on the compressive and tension sides of the wall. In a deformed state of the wall, the friction between the wall and the airbags on the tension side of the wall can promote an increase in lateral force. This effect resulted larger for displacement in the positive loading direction, because the pressure in the airbags on the north side was higher. Thanks to additional tests on the wall TUD\_COMP-27 after the standard testing procedure was applied, a correction function was determined to take into account the increase in lateral force due to the friction effect. This function is used to provide a revised capacity curve. It should be noted that this effect is negligible for negative displacements (for which the pressure on the tension side was small), thus the correction function is applied only for positive displacements.

### 3 EXPERIMENTAL RESULTS

The experimental results of quasi-static cyclic out-of-plane tests are reported in terms of capacity curve (lateral force versus mid-point displacement, Figure 2 and Figure 3), initial stiffness, lateral force at onset cracking (evaluated considering the first visible decreasing in stiffness), and crack pattern at the end of the test (Table 3).

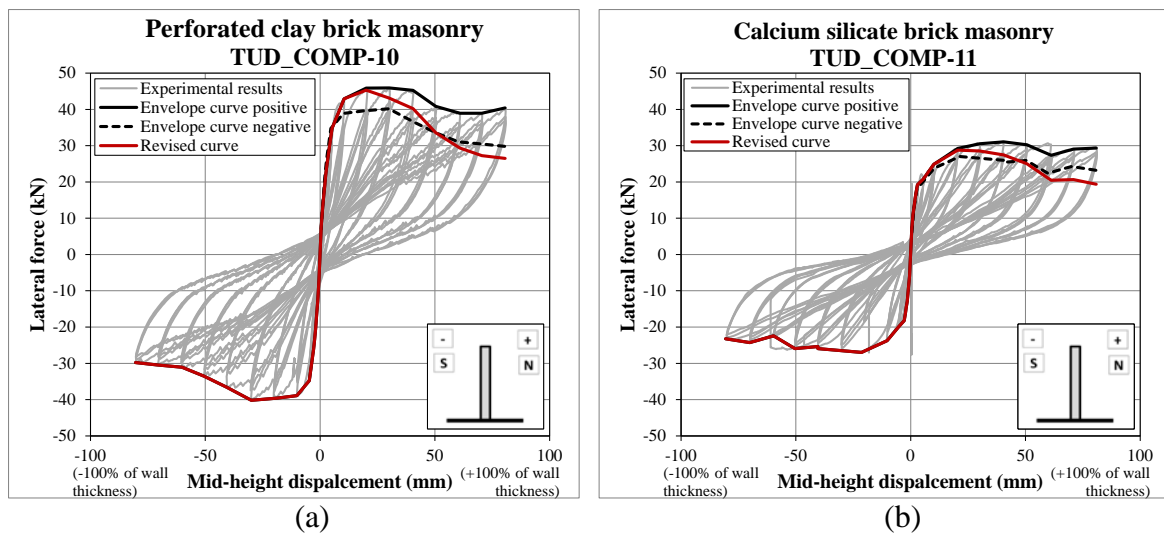


Figure 2: Capacity curve for walls (a) TUD\_COMP-10, (b) TUD\_COMP-11.

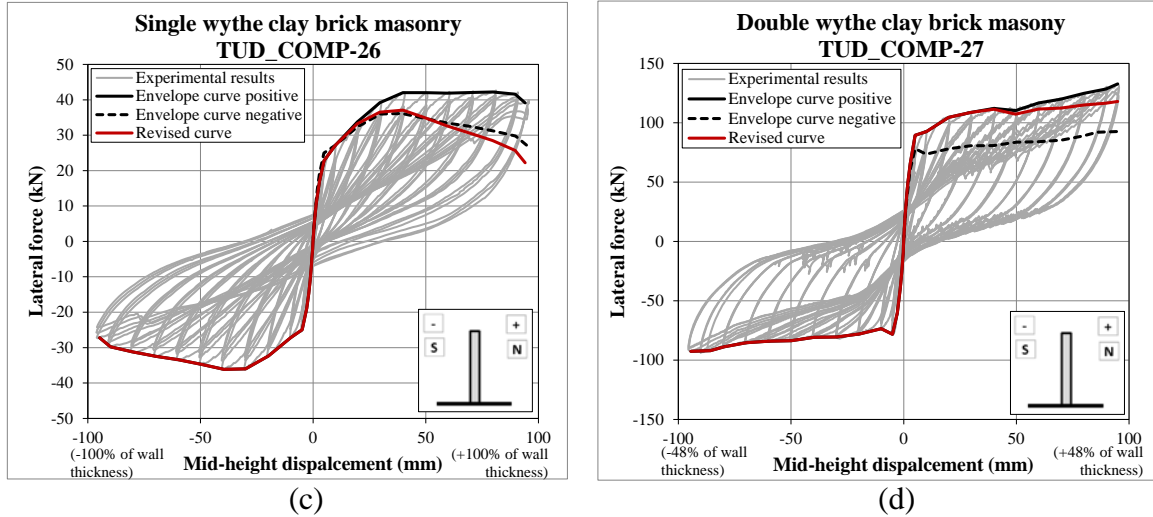


Figure 3: Capacity curve for walls (a) TUD\_COMP-26, (b) TUD\_COMP-27.

Sample name	Masonry type	Initial stiffness $K_{in}$ (N/mm)	Lateral Force		
			$F_{cr}$ (kN)	$F^+$ (kN)	$F^-$ (kN)
TUD_COMP-10	Single wythe perforated clay brick	12.8	34.8	45.3*	-40.2
TUD_COMP-11	Single wythe calcium silicate brick	12.0	18.2	28.9*	-27.0
TUD_COMP-26	Single wythe solid clay brick	9.6	20.0	37.1*	-36.1
TUD_COMP-27	Double wythe solid clay brick	41.4	78.3	89.5*	-78.3

\* Revised value to account for the lateral force increment due to the friction effect.

Table 3: Overview of experimental results in terms of initial stiffness  $K_{in}$ , lateral force at onset of cracking  $F_{cr}$  and maximum lateral force for positive,  $F^+$ , and negative,  $F^-$ , displacements.

The initial stiffness obtained experimentally is determined as the linear regression of the lateral force versus mid-point displacement curve of the first cycle in the elastic phase. For the wall TUD\_COMP-10 and TUD\_COMP-11 the first cycle is characterized by an imposed displacement of 0.5 mm, while for the specimens TUD\_COMP-26 and TUD\_COMP-27 it is equal to 0.1 mm. In order to compare the stiffness degradation for single wythe walls, the stiffness is evaluated at imposed displacement of 0.5 and 1 mm. The calcium silicate brick masonry wall shows stiffness degradation almost two times higher than the other single wythe walls.

Figure 2 and Figure 3 show the out-of-plane behavior of the walls in terms of capacity curve. For the positive loading direction the envelope curve has been revised accounting for the friction effect (see Section 2). By comparing the revised envelope curve for the positive displacement and the envelope curve for the negative displacement, a good agreement is generally found for the two directions. The maximum lateral force of the single wythe walls (TUD\_COMP-10,-11,-26, Figure 2 and Figure 3a), obtained with reference to the revised envelope curve, is slightly higher in the positive loading direction. This can be linked to the damage evolution which occurs first in the positive loading direction, being this the first loading direction in every cycle. Considering the double wythe wall TUD-COMP-27 (Figure 3b) the influence of damage evolution on the basis of the loading direction is more evident than in the other specimens; this may be caused by the difference in wall thickness. In terms of lateral force capacity, the calcium silicate brick masonry wall records the lowest capacity, while the

double wythe clay masonry wall shows a lateral force capacity almost two times higher than both the single wythe clay masonry walls (Table 3).

The post-peak behavior is characterized by a plateau at a force approximately equal to the maximum lateral force. In the case of the single wythe walls, a slight reduction in force is observed, while for the double wythe wall a slight increase is observed. However it should be pointed out that the single wythe walls have been tested for a mid-point displacement equal to approximately 90% of wall thickness, while in the case of double wythe wall a displacement of 50% of the wall thickness was imposed. Griffith and Vaculik [12] report that the presence of a constant plateau in the post-peak phase of the capacity curve can be caused by the redistribution of the diagonal bending moment acting along the diagonal cracks to a horizontal bending moment acting along the vertical edges. The qualitative agreement of post-peak behavior trends suggests that the lateral boundary conditions adopted in this study can provide the same constraints as given by return walls as adopted in [12].

#### 4 ANALYTICAL CALCULATIONS

In this section the lateral force of the tested specimens is evaluated according to the Eurocode 6 [5], the Australian Standard [6] and the simplified macroblock approach proposed by Vaculik and Griffith [7-8]. All the methods have been applied by considering the mean material properties as reported in Table 2 and excluding design coefficients. Moreover, all the proposed methods are designed for single wythe walls and consequently the double wythe specimen TUD\_COMP-27 is excluded from the comparison.

The Eurocode 6 formulation provides an estimate of the elastic bending moment and consequently the obtained lateral force is compared with the experimental force at onset of cracking  $F_{cr}$ . The prediction is based on a tabulated coefficient depending on the ratio between the flexural strengths of masonry  $f_{x1}/f_{x2}$ , on the aspect ratio of the wall and on the boundary conditions. Note that in this comparison, it is assumed that the flexural strength for a plane of failure perpendicular to the bed joints  $f_{x1}$  is equivalent to the flexural bond strength  $f_w$ . For the comparison, the formulation proposed by Eurocode 6 is applied both in the case of hinged connections at all sides of the wall and in the case of clamped connections at all sides of the wall; this results in lower and upper bounds of the lateral capacity for the tested walls respectively (Figure 4a). Although the Eurocode 6 formulation is simple, its application requires a precise knowledge of both the flexural strengths of masonry that is not always possible for existing structures.

The Australian standard, based on the virtual work method, provides an estimate of the lateral force capacity starting from the evaluation of the horizontal and diagonal bending moments capacities according to the predicted crack pattern. The Australian standard considers only walls with an half-overlap bond pattern; on the basis of this assumption and considering the units and joints dimensions, the standard defines the slope of diagonal cracks, thus the predicted crack pattern. The method proposed by the Australian standard provides an underestimation of the lateral force capacity between 17 and 56% (green column in Figure 4b). Generally, the formulation is not able to predict the crack pattern experimentally observed and in the majority of the cases a crack pattern with a central vertical crack is considered rather than the one with a horizontal crack. If the predicted and experimental crack patterns are in agreement a good prediction can be obtained as for the case of wall TUD\_COMP-11. The error in the crack pattern prediction made by the Australian standard is given by the slope of the diagonal cracks. In fact, in the experiments the diagonal cracks do not propagate exactly from the corner as it is assumed in the standard. The same finding in the crack pattern was reported also by Griffith and Vaculik in [12]. The underestimation of the lateral force capacity may be caused also by other reasons such as the absence of a contribution considering the influence of



the vertical bending moment with respect to the horizontal cracks and the influence of the overburden (see also Section 5). Despite the limit in its application, the Australian standard formulation is nowadays the most accurate model formulation to estimate the lateral force capacity of two-way spanning walls.

The simplified macroblock approach assumes, differently from the Australian standard, that the wall lateral load resistance is obtained considering the independently acting resistance sources of rocking and friction. It assumes the wall as already cracked, i.e. masonry flexural strength set to zero. The model, using a nonlinear static analysis, provides the entire load-displacement behavior of the wall up to the point of collapse, i.e. instability displacement, as comprised by rigid body rocking source and horizontal bending friction source, considered as acting independently. The model considers the wall as a series of vertically spanning strips held together by kinematic compatibility dictated by the shape of the collapse mechanism. Similarly to the Australian standard, this method is formulated only for half-overlap bond pattern. This method provides an underestimation in lateral force capacity between 54 and 63% (purple column in Figure 4b). The underestimation is generally higher with respect to the one provided by the Australian standard method because the macroblock considers the same crack pattern as the standard and zero masonry flexural strength. The Australian standard considers a minimum value of 0.2 MPa of flexural strength if no experimental data are available. Due to the difficult evaluation of the flexural strength of masonry in existing masonry buildings and the formulation of the instability displacement, the simplified macroblock approach represents an interesting model to be used in engineering practice for assessing the two-way bending failure mechanism. In the case of Dutch URM buildings, for which the proposed tests were carried out, the assumption of zero flexural masonry strength may be too conservative in the case of clay brick masonry, but appropriate for calcium silicate masonry [13].

A kinematic limit analysis by assuming the one-way rigid block mechanism is performed (red column in Figure 4b) in comparison with the formulations proposed by Australian standard and the simplified macroblock approach. Comparing the one-way rigid block method and the experimental results in terms of lateral force capacity, an underestimation between 62 and 74% is obtained. Comparing the results obtained by the Australian standard and the one obtained by the one-way rigid block method an increase of 16 to 45% in terms of estimated capacity is obtained, while considering the simplified macroblock approach an increase of 6 to 18% is obtained. However, considering the complexity of both methods, the amount of input parameters needed and the overestimation in terms of capacity with respect to the experimental results, this increase in estimated capacity is still limited. This emphasizes once more the need of an appropriate formulation to estimate the lateral force capacity of two-way spanning walls.

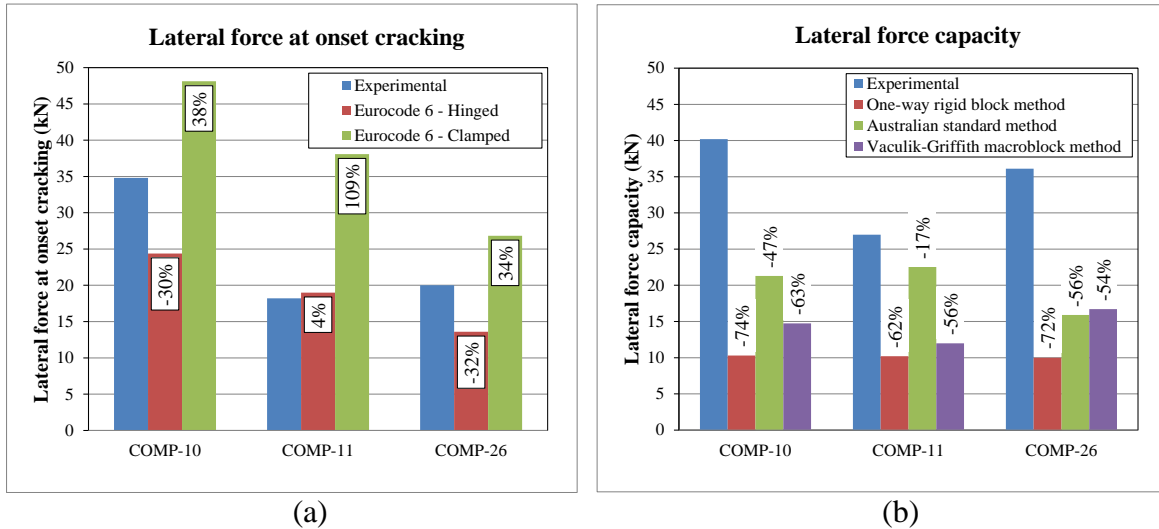


Figure 4: Comparison between experimental results and analytical predictions by (a) Eurocode 6 (b) one-way rigid block method, Australian standard method and Vaculik-Griffith macroblock method. Percentage value indicates the error of each method with respect to the experimental result.

## 5 PARAMETRIC STUDY

In the previous section various methods to estimate the lateral force capacity of two-way spanning walls subject to out-of-plane failure have been analyzed in comparison with experimental results. Among others the method proposed by the Australian Standard looks promising because if the correct crack pattern is considered then the predictions get closer to the experimental results. However, the comparison with experimental results highlighted the need of improving the current formulation. For this purpose, in this section a parametric study is performed considering the method proposed by the Australian Standard. The study has been performed focusing on the parameters that mostly influence the lateral force capacity, namely: the flexural strength of masonry ( $f_w$ ), the overburden ( $\sigma$ ), the vertical edges rotational restraint coefficient ( $R_f$ ), the aspect ratio ( $L_d/H_d$ ), and the unit size. The tests presented in this paper (Section 3) and the similar tests performed by Griffith and Vaculik [12] on clay brick masonry walls No. 1 and 2 (here named G1 and G2) are considered. It should be noted that the variation of all the presented parameters is related to the bending capacity of the wall  $w$  expressed in terms of pressure, which is the lateral force capacity of the wall  $F$  divided by the area of the wall.

The influences of the flexural strength of masonry and of the overburden on the bending capacity of the wall are firstly investigated. Generally, the bending capacity of the wall significantly increases by increasing the flexural strength of masonry, while it is almost constant by increasing the overburden. The case of a wall having an aspect ratio of 1.48, unit size of 210x50x100-mm and vertical edges rotational restraint coefficient equal to zero is presented in Figure 5a. In this specific case, the increase of  $f_w$  from 0.1 to 0.2 MPa results in an increase in the bending capacity of approximately +35%. In the same case, the increase in overburden from 0 to 0.1 MPa produces an increase in bending capacity of maximum +14%. For comparison, the experimental results of wall TUD\_COMP-26, characterized by an overburden of 0.06 MPa and in agreement with the assumptions of the presented case, is also shown in Figure 5a. As already discussed in Section 4, its experimental bending capacity is more than two times higher than the one estimated by the Australian standard.

The bending capacity of the wall estimated with the method proposed by the Australian standard is hardly influenced by the overburden. This trend is in contrast with experimental results reported by Griffith and Vaculik [12]. To highlight this difference, in Figure 5b the Australian standard method is compared to the experimental results of walls G1 and G2; the two tests have the same geometry and similar material properties but two different overburden values of 0.1 and 0 MPa, respectively. An increase in overburden experimentally results in an increase in bending capacity of +57%. On the contrary, the formulation by the Australian standard accounts only for a limited increase in bending capacity (+17%), that is a third of the one experimentally obtained.

The supports to the vertical edges can provide a different degree of rotational restraint, which in the method proposed by the Australian standard is considered with the vertical edges rotational restraint coefficient  $R_f$ . Generally, by increasing the rotational restraint from hinged constraints ( $R_f=0$ ) to clamped constraints ( $R_f=1$ ), the bending capacity significantly increases. The case of a wall having aspect ratio of 1.48, unit size of 210x50x100-mm and an overburden of 0.06 MPa is presented in Figure 5c. In this specific case, the variation from hinged constraints ( $R_f=0$ ) to partially clamped constraints ( $R_f=0.5$ ) produces an increase in bending capacity between +35 and +48%, while the variation from hinged constraints ( $R_f=0$ ) to clamped constraints ( $R_f=1$ ) produces an increase in bending capacity between +70 and +97%. The evaluation of the vertical edges rotational restraint coefficient can be quite difficult in in-situ conditions. Consequently, limiting the influence of this coefficient by standardizing the rotational restraint for some typical as-built conditions could be useful in the calculation of existing masonry buildings.

The influence of unit geometry and aspect ratio of the wall is finally investigated. Generally, the bending capacity significantly decreases with the increase in the aspect ratio of the wall, while it increases with the increase in wall thickness. The case of a wall having an overburden of 0.06 MPa, a flexural strength of masonry equal to 0.15 MPa and a vertical edge rotational restraint coefficient equal to zero is presented in Figure 5d. In this specific case, no significant difference is found increasing the unit height from 50 to 70 mm, typical height values for Dutch masonry units. In the same presented case, the increase in wall thickness from 100 to 110 mm produces an increase in bending capacity of approximately +20%, independently on the aspect ratio of the wall. Additionally, it should be noticed that the Australian standard method does not consider any difference in the formulation between hollow (named cored in the standard) and solid bricks. Comparing the experimental results of the hollow clay brick masonry wall TUD\_COMP-10 and the solid clay brick masonry wall TUD\_COMP-26 a variation in lateral force capacity of 10% is found, which can be related to a slightly different aspect ratio of the wall and different value of flexural strength of masonry.

Additionally, it has to be pointed out that in this parametric study of the influence of the flexural strength of the units and of the weight per unit volume of masonry is not addressed, because no influence on the bending capacity is found for the analyzed cases.

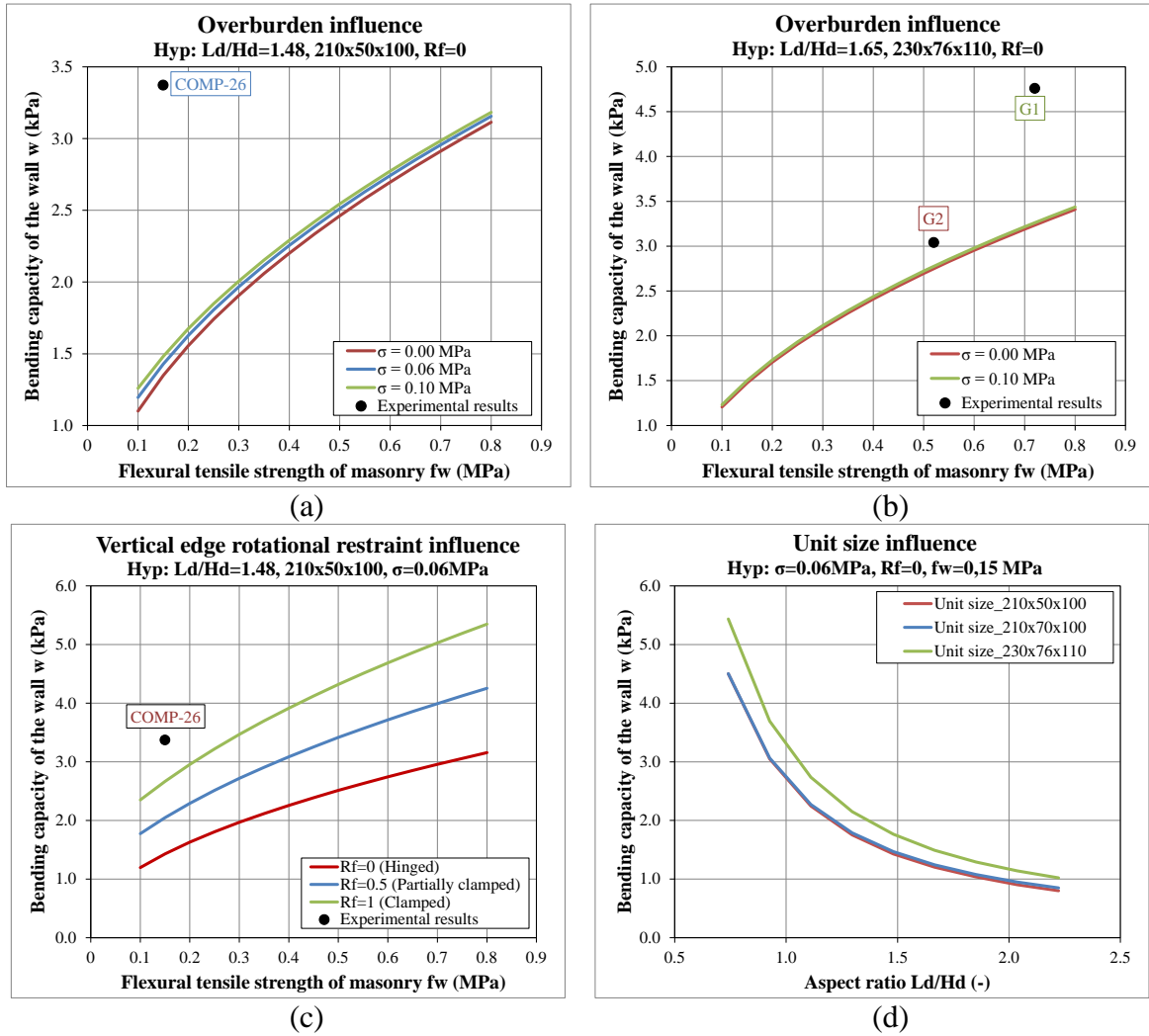


Figure 5: Influence of material and geometrical properties on the bending capacity of the wall by the Australian standard formulation. (a) influence of the overburden  $\sigma$  and masonry flexural strength  $f_w$  - first case, (b) influence of the overburden  $\sigma$  and masonry flexural strength  $f_w$  - second case, (c) influence of vertical edge rotational restraint coefficient  $R_f$  and (d) influence of unit size and wall aspect ratio  $L_d/H_d$ .

Figure 6 shows a comparison between the experimental results and the Australian standard formulation by considering the case of partially clamped constraints ( $R_f=0.5$ , as considered by Griffith [12]) and hinged constraints ( $R_f=0$ ). The markers represent the experimental results, while the curves show the analytical. Each curve is obtained using the material properties and the overburden characteristic of each wall. Figure 6 shows that to obtain a good agreement between experimental and analytical results, it is not effective to modify the vertical edges rotational restraint coefficient as suggested by Griffith [12], but it is important to consider the influence of overburden and to correctly estimate the experimental crack pattern. In fact, comparing the walls G1 and G2, having the same boundary conditions, similar characteristics but different overburden, a good agreement with the standard prediction is found considering different values of  $R_f$ . Additionally, by comparing the two estimated curves for wall TUD\_COMP-11 with a low overburden, a value closer to the experimental one is obtained independently on the vertical edge rotational restraint coefficient; only for this case the estimated and experimental crack pattern are in agreement.

Concluding, the parameters that mostly influence the bending capacity of the wall within the Australian standard are the vertical edges rotational restraint coefficient, the flexural

strength of masonry, the aspect ratio and the wall thickness. While the latter two parameters are easy to assess, the former two are not. Consequently, to better study the real influence of these parameters as well as the influence of the parameters only marginally considered by the standard, in particular the overburden, an experimental campaign investigating different boundary conditions, wall geometry and masonry types is needed.

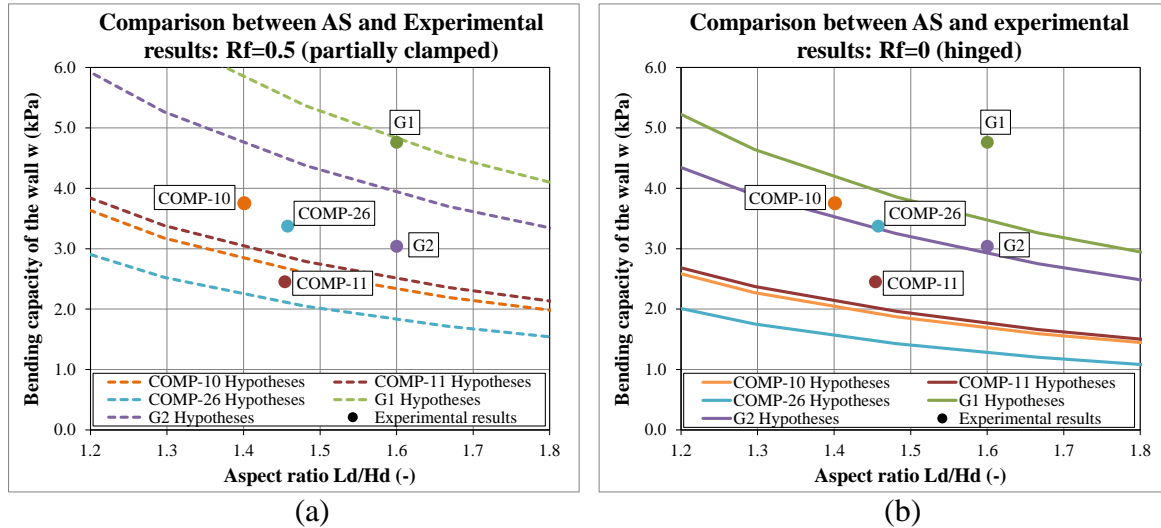


Figure 6: Comparison between Australian standard formulation and experimental results considering (a) vertical edges rotational restraint coefficient  $R_f=0.5$  (b) vertical edges rotational restraint coefficient  $R_f=1$ .

## 6 SUMMARY AND CONCLUSIONS

Four full-scale unreinforced masonry (URM) walls were subjected to quasi-static out-of-plane cyclic tests in order to investigate the two-way out-of-plane bending failure mechanism. The walls, characterized by different materials, were tested applying the same overburden and boundary conditions. The tests were performed using an airbag system and in displacement control.

By observing the experimental results the following conclusions can be drawn:

- An almost constant post-peak strength plateau was found. The agreement of post-peak behavior with the one found by Griffith and Vaculik [12] suggests that the adopted lateral boundary conditions well represents the restraint obtained by the presence of return walls.
- At the final stage, the typical two-way bending failure mechanism was observed. All the tested walls were characterized by two main diagonal step-wise cracks developed starting next to the corners and orientated towards the central part of the wall, an horizontal crack along the bed joint at mid-height connecting the diagonal cracks and two horizontal cracks formed at the first and last mortar bed joint.

By comparing the experimental and analytical results the following conclusions can be drawn:

- The formulation proposed by Eurocode 6 can be applied only to estimate the lateral force at the onset of cracking, which is generally substantially lower than the lateral force capacity obtained in the damaged (but stable) configuration. For the considered cases, the formulation provides upper and lower bounds for the estimation of the lateral capacity, because it considers only the condition of four clamped sides and the

condition of four hinged sides. Moreover, in order to have reliable predictions a precise knowledge of both the flexural strengths of masonry is needed.

- The formulation proposed by the Australian standard provides an underestimation in the lateral force capacity between 17 and 56%. The best prediction was obtained when the standard correctly predicts the crack pattern with the horizontal mid-height crack. The incorrect crack pattern often predicted by the standard is due to the incorrect assumption of diagonal cracks propagating exactly from the corners. Additionally, other factors appear to play a role within the assessment of the lateral force capacity (e.g. overburden). For this reason, a parametric study has been performed considering the Australian standard formulation to highlight its current limitations.
- The simplified macroblock approach proposed by Vaculik and Griffith, neglecting the flexural strength of masonry, provides a larger underestimation of the lateral force capacity with respect to the Australian standard. The underestimation is between 54 and 63%. Due to the difficult evaluation of the flexural strength of masonry in existing masonry buildings and due to the provision of instability displacement, the simplified macroblock approach represents an interesting model to be used in engineer practice for assessing the two-way bending failure mechanism but at the moment it provides an underestimation of the same order of the one obtained by assuming a one-way vertical spanning wall.
- All the proposed formulations for two-way bending are designed for single wythe walls and no formulation is available for multi wythe walls. Additionally, the Australian standard formulation and simplified macroblock approach are only available for half-overlap masonry.

By analyzing the Australian standard formulation through a parametric study, the following conclusions can be drawn:

- The parameters that mostly influence the bending capacity of the wall are the vertical edges rotational restrain coefficient, the flexural strength of masonry, the aspect ratio and the wall thickness. On the contrary, variations of the flexural strength of unit and of the weight per unit volume of masonry do not lead to variation in terms of capacity.
- The bending capacity of the wall significantly increases with the increase of: flexural strength of masonry, vertical edges rotational restrain coefficient and thickness of the wall. The bending capacity of the wall significantly increases also with the decrease of the aspect ratio of the wall.
- The analytical model does not properly account for the influence of the overburden, which experimentally is proven to be significant.
- The Australian standard formulation does not consider any difference between hollow (named cored in the standard) and solid brick. This is in agreement with the experimental tests reported in this paper.

As highlighted by the interpretation of the experimental findings and the evaluation of available analytical models, the formulation of an improved analytical model to capture the two-way bending failure mechanism is needed. Nowadays, the most accurate formulation is the one provided by the Australian standard. In order to improve the method and to extend it also to multi wythe walls, additional formulations for the definition of the crack pattern and an experimental campaign investigating different boundary conditions, wall geometry and masonry types are needed.

## ACKNOWLEDGEMENTS

This research was funded by NAM under contract numbers UI46268 “Physical testing and modelling – Masonry structures Groningen” and UI63654 “Testing program 2016 for Structural Upgrading of URM Structures”, which is gratefully acknowledged. Part of this work was performed in cooperation with the engineering firm ARUP and the research center EUCENTRE.

## REFERENCES

- [1] G. Magenes, Masonry building design in seismic areas: recent experiences and prospects from a European standpoint. *Proc. 1<sup>st</sup> European Conference on Earthquake Engineering and Seismology*, Geneva, 2006.
- [2] G. Ravenshorst, F. Messali, *Out-of-plane tests on replicated masonry walls*. Report version 4 of 30-05-2016, Delft University of Technology, 2016.
- [3] F. Messali, G. Ravenshorst, R. Esposito, J. Rots, Large-scale testing program for the seismic characterization of Dutch masonry walls. *Proc. 16<sup>th</sup> World Conf. on Earthquake Engineering*, Santiago, 2017.
- [4] M. Damiola, R. Esposito, G.J.P. Ravenshorst, *Quasi-static cyclic out-of-plane tests on masonry components 2016/2017*. Report number C31B67W3-5 version 01 of 05-12-2017, Delft University of Technology, 2017.
- [5] EN 1996-1-1: Eurocode 6: design of masonry structures. Part 1-1: general rules for reinforced and unreinforced masonry structures. 2013.
- [6] AS 3700-2011: Australian Standard: masonry structures. 2011.
- [7] J. Vaculik, *Unreinforced masonry walls subject to out-of-plane seismic actions*. PhD Thesis, The University of Adelaide, Adelaide (AU), 2012.
- [8] J. Vaculik, M.C. Griffith, Out-of-Plane load-displacement model for two-way spanning masonry walls. *Engineering Structures*, 141, 328-343, 2017.
- [9] S. Jafari, R. Esposito, *Material tests for the characterisation of replicated solid clay brick masonry*. Report number C31B67WP1-12 version 01 of 12-08-2017, Delft University of Technology, 2017.
- [10] S. Jafari, R. Esposito, *Material tests for the characterisation of replicated calcium silicate element masonry*. Report number C31B67WP1-11 version 01 of 11-08-2017, Delft University of Technology, 2017.
- [11] M.C. Griffith, J. Vaculik, N.T.K. Lam, J. Wilson E. Lumantarna, Cyclic testing of unreinforced masonry walls in two-way bending. *Earthquake Engineering and Structural Dynamics*, **36**(6), 801-821, 2007.
- [12] M.C. Griffith, J. Vaculik, Out-of-Plane Flexural Strength of Unreinforced Clay Brick Masonry Walls. *TSM Journal*, **25**(1), 53-68, 2007.
- [13] S. Jafari, J. Pawlowicz, R. Esposito, *Material characterisation of existing masonry for URM abacus*. Report number C31B67WP1-14 version 01 of 18-01-2018, Delft University of Technology, 2018.